This article has been accepted for inclusion in a future issue of this journal. Content is final as presented, with the exception of pagination.



# Balanced Six-Port Reflectometer With Nonmatched Power Detectors

Kamil Staszek

***Abstract*— In this article, a six-port reflectometer is proposed, which utilizes nonmatched power detectors. In the presented solution, the signals reflected from power detectors are efficiently used to obtain a signal flow required for correct measurements. As a consequence, impedance matching networks for power detectors are no longer needed. Simultaneously, due to its balanced topology, the developed six-port exhibits advantageous measurement conditions and theoretically ideal matching at both its input and measurement ports. To experimentally validate the proposed concept, a six-port reflectometer operating at 2.4 GHz is designed, manufactured, and utilized in reflection coefficient measurements. The obtained results are consistent with the values measured using a commercial vector network analyzer. For additional verification, the impact of power detectors' asymmetry is investigated theoretically and experimentally.**

***Index Terms*— Balanced network, impedance match, power detector, reflection coefficient, six-port reflectometer.**

## I. Introduction

MULTIPORT measurement technique, originally developed as an alternative for vector network analyzers [1], [2], becomes more and more attractive in contemporary microwave electronics [3]. Due to simple circuitry, good linearity, and power efficiency, multiport measurement systems have found a wide range of applications, in which a vector measurement of microwave signals is needed. Such systems are not only used in direct measurement of scattering parameters [4], [5] but also in various permittivity sensors [6], [7], radars [8], [9], and communication systems [10], [11]. Moreover, due to the above advantages, six-port reflectometers are also used in the optical frequency range [12], [13].

A key element of the multiport measurement system is a passive multiport power distribution network, which distributes microwave signal from excitation port to device under test, the *S*-parameters of which are subject to measure, and to power detectors. By an appropriate design of such a multiport network, simple scalar power measurement can be transformed into a vector value [14]. The power distribution scheme together with the number of used power detectors and their measurement uncertainty determines the multiport measurement system's performance [15]. The most common group of multiport utilized in such measurements is six-ports, as they have the minimum number of ports ensuring unambiguous measurement. Namely, they have an exciting port, measurement port, and four ports with power detectors connected, among which three ones are directly used for the measurement, whereas the fourth one serves for reference power measurement [16]. Nevertheless, six-ports having four power detectors used directly for the measurement with no reference power measurement capability are also reported [17]. They exhibit a distinctly better measurement uncertainty with no compensation of the signal source's power level instability as a tradeoff [15]. It is also worth noting that, due to rapid development of the multiport technique, networks with various numbers of ports and power detectors have been reported, starting from four-ports with only two power detectors [18] to networks with eight [19] and nine [20] power detectors providing enhanced measurement uncertainty.

As mentioned above, the inner signal distribution in the multiport network has a major impact on the measurement uncertainty. Therefore, the used power detectors must be well-matched, as the undesired signals reflected from detectors' input ports interfere with the desired signals distributed by the multiport network, leading to impairment of the measurement system's performance. If these reflections are relatively small, they constitute a source of a systematic error that can be suppressed by a calibration procedure [21], [22]. Nevertheless, each deterioration of the power distribution affects the measurement uncertainty [15]. Furthermore, large reflections can lead to a severe impairment under which the measurement is no longer possible. On the other hand, the multiport systems are intended for low-cost solutions; therefore, they are often developed in conjunction with simple diode power detectors, which inherently exhibits poor impedance match [23]. As a consequence, dedicated impedance matching networks need to be utilized, which increases design effort and increases the circuit's size [24].

To overcome this limitation, a new approach to six-port reflectometers design is proposed in this article. It incorporates a balanced six-port power division network with four nonmatched power detectors and allows for eliminating the need for impedance matching networks' application for power detectors. Simultaneously, due to the balanced topology of the six-port network, it exhibits theoretically ideal impedance match at its both feeding port and the measurement port, to which device under test is connected. It is shown that the signals reflected from power detectors' input ports can be efficiently used to obtain the inner signals propagation scheme required in multiport measurement systems. The provided

Manuscript received March 11, 2021; revised May 24, 2021; accepted July 1, 2021. This work was supported by Norway Grants 2014–2021 through the National Centre for Research and Development.

The author is with the Department of Electronics, AGH University of Science and Technology, 30-059 Krakow, Poland (e-mail: kamil.staszek@agh.edu.pl).

Color versions of one or more figures in this article are available at https://doi.org/10.1109/TMTT.2021.3101701.

Digital Object Identifier 10.1109/TMTT.2021.3101701

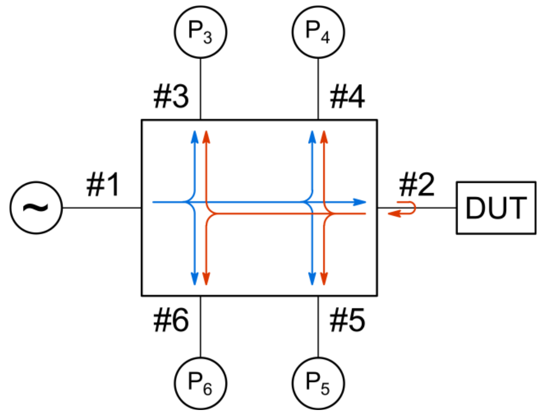


Fig. 1. Simplified signal flow in the classic six-port reflectometer utilizing matched power detectors.

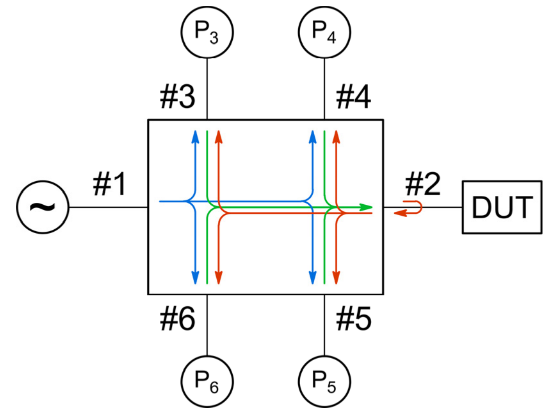


Fig. 2. Simplified signal flow in the proposed balanced six-port reflectometer with nonmatched power detectors.

theoretical investigation reveals that even power detectors with significant return losses can be used in the proposed six-port with no deterioration of the system's performance. For experimental verification, the proposed balanced six-port reflectometer with four nonmatched power detectors is designed and manufactured. It provides very good measurement conditions, which fully confirms theoretical expectations. The obtained reflection coefficient measurement error related to a commercial vector network analyzer does not exceed the value of 0.0122 at the center frequency. Finally, the reflectometer's performance is examined with an intentional impairment of a single power detector. It is shown that, even with a significant deterioration of a single power detector, the proposed six-port reflectometer operates correctly.

This article is organized as follows. First, the general principle of operation for conventional six-port reflectometers is described in Section II. Section III reveals the idea of the proposed balanced six-port reflectometer and provides a theoretical investigation. In Section IV, the six-port's network design is reported, whereas Section V presents the measurement setup incorporating the developed six-port together with its calibration and measurement results. Section VI describes the impact of power detectors' asymmetry on the measurement performance, whereas Section VII concludes this article.

## II. Principle of Operation for Six-Port Reflectometers

The classic six-port reflectometer is presented in Fig. 1. Its major component is a six-port passive network, which distributes the signal from port #1 to its all remaining ports, i.e., to port #2 with the connected device under test, and to ports #3–#6, to which power detectors $P_3$–$P_6$ are connected, respectively. The signal incident to the device under test reflects from it according to its reflection coefficient $\Gamma$ and is distributed backward to ports #3–#6. As a consequence, each power detector measures the power of a sum of two signals, among which one is linearly related to the measured reflection coefficient $\Gamma$, whereas the second one serves for reference. Therefore, the power $P_i$ measured by the $i$th detector ($i = 3, 4, 5, 6$) can be expressed as

$$P_i = q_i |1 + A_i \Gamma|^2 \tag{1}$$

where $q_i$ and $A_i$ are systems' constants needed to be determined in a calibration procedure before measurements.

As it is shown in [1], the reflection coefficient $\Gamma$, being a solution of the set of equations (1), can be interpreted geometrically as an intersection point of four circles. These circles have their centers in points $c_i$ defined as

$$c_i = -\frac{1}{A_i} \tag{2}$$

whereas their radii $r_i$ are equal to

$$r_i = \sqrt{\frac{P_i}{q_i |A_i|^2}}. \tag{3}$$

Having determined the circle centers' distribution and the power measurement uncertainty, the uncertainty of the reflection coefficient measurement can be calculated with the use of a method reported in [15]. From the measurement uncertainty perspective, it is crucial to preserve the signal propagation indicated schematically in Fig. 1. Therefore, the utilized power detectors $P_3$–$P_6$ should provide a possibly good impedance match. Otherwise, signals reflected from power detectors interfere with desired signals marked blue and red in Fig. 1. This, in turn, changes the location of particular circle centers $c_i$, leading to an impairment of the entire reflectometer's measurement uncertainty. Hence, in classic six-port reflectometers that utilize simple diode power detectors, which are inherently poorly matched, additional matching networks must be applied.

## III. Theoretical Investigation on the Proposed Balanced Six-Port Reflectometer With Nonmatched Power Detectors

The abovementioned poor impedance match of diode power detectors can be effectively utilized in the proposed concept of the balanced six-port reflectometer utilizing nonmatched power detectors presented in Fig. 2. As seen, the components' arrangement is identical to the classic solutions; however, the inner signal distribution is different. In the proposed balanced six-port reflectometer, the excitation signal from port #1 of the six-port network is distributed to power detectors only, i.e., to ports #3–#6 (blue lines in Fig. 2). Port #2 with the

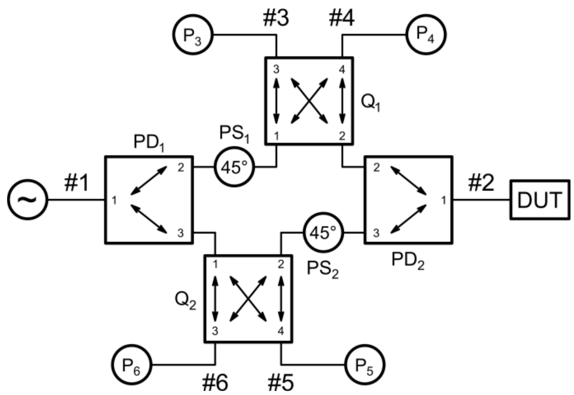


Fig. 3. Schematic of the proposed balanced six-port reflectometer with nonmatched power detectors.

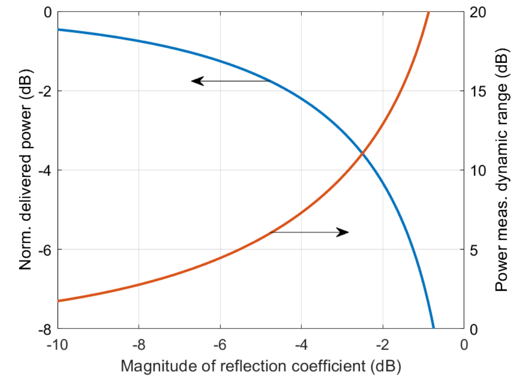


Fig. 4. Impact of the reflection coefficient's magnitude of power detectors on the normalized delivered power and the power measurement dynamic range in the proposed six-port reflectometer.

device under test is isolated with respect to port #1. However, due to the poor impedance match of the power detectors $P_3$–$P_6$, the signals reflected from them propagate to DUT (green lines in Fig. 2). Next, they are reflected according to the DUT's reflection coefficient $\Gamma$ and, finally, are delivered to the power detectors $P_3$–$P_6$ (red lines in Fig. 2). Also, in this case, the power measured by the power detectors can be expressed using exactly the same relation (1) as for the classic reflectometers. Simultaneously, as it is described further in this section, the entire reflectometer can exhibit theoretically ideal impedance match at ports #1 and #2, and an advantageous circle centers' distribution leading to low measurement uncertainty.

To realize the above concept, a balanced six-port reflectometer illustrated in Fig. 3 can be proposed. Its major component is a six-port network composed of two equal-split power dividers $PD_1$ and $PD_2$, two phase shifters $PS_1$ and $PS_2$ providing a phase shift equal to 45°, and two 3-dB/90° directional couplers $Q_1$ and $Q_2$. The six-port network provides a uniform power split from feeding port #1 to all power detectors at ports #3–#6, with appropriate phase shifts, which will be discussed further in this section. Moreover, excitation port #1 and measurement port #2 are isolated; however, the transmission between these ports occurs if four identical power detectors exhibiting a reflection coefficient $\Gamma_D$ of distinct magnitude are connected to ports #3–#6. This simultaneously ensures an ideal impedance match at ports #1 and #2. The power measured by power detectors equals

$$P_3 = \frac{P_{\text{GEN}}}{4}\left(1 - |\Gamma_D|^2\right) \cdot |1 - \Gamma_D \Gamma|^2 \tag{4a}$$

$$P_4 = \frac{P_{\text{GEN}}}{4}\left(1 - |\Gamma_D|^2\right) \cdot |1 + \Gamma_D \Gamma|^2 \tag{4b}$$

$$P_5 = \frac{P_{\text{GEN}}}{4}\left(1 - |\Gamma_D|^2\right) \cdot |1 + j\Gamma_D \Gamma|^2 \tag{4c}$$

$$P_6 = \frac{P_{\text{GEN}}}{4}\left(1 - |\Gamma_D|^2\right) \cdot |1 - j\Gamma_D \Gamma|^2 \tag{4d}$$

where $P_{\text{GEN}}$ is the power incident to port #1 of the reflectometer. As it is seen, (4) can be expressed using the general form (1), where

$$q_i = \frac{P_{\text{GEN}}}{4}\left(1 - |\Gamma_D|^2\right) \tag{5}$$

and

$$A_3 = -\Gamma_D \tag{6a}$$

$$A_4 = \Gamma_D \tag{6b}$$

$$A_5 = j\Gamma_D \tag{6c}$$

$$A_6 = -j\Gamma_D. \tag{6d}$$

The coefficients $A_i$ specified by (6) can now be used to calculate circle centers $c_i$, as given in (2). It is clearly seen that all circle centers share identical magnitudes, which is inversely proportional to the magnitude of the power detectors' reflection coefficient. On the other hand, their phases differ by 90° due to the quadrature phase shift of the couplers $Q_1$ and $Q_2$, and the phase shifters $PS_1$ and $PS_2$. Hence, a uniform circle centers' distribution is obtained, which leads to a low measurement uncertainty [15]. Simultaneously, for each power detector, the coefficients $q_i$ are equal. Therefore, each power detector will operate at comparable power levels.

Since, in the proposed balanced six-port reflectometer, the nonmatched power detectors are applied, their impact on the reflectometer's performance has to be analyzed. First, it must be underlined that a worse impedance match of the power detector decreases the delivered power $P_D$, i.e., the power measured by the detector with respect to the power incident to the detector $P_I$. The ratio of these values is equal to

$$\frac{P_D}{P_I} = 1 - |\Gamma_D|^2 \tag{7}$$

and is illustrated in Fig. 4 (blue curve). It is obvious that increasing the magnitude of the reflection coefficient leads to a drop of the power efficiently measured by the detector. Nevertheless, it is worth noting that power detectors used in contemporary electronics exhibit the power dynamic range not worse than 20 dB but can also reach 40 dB or more. Therefore, a loss of few dB does not constitute a distinct impairment.

Apart from the drop of the delivered power $P_D$ with respect to the incident power $P_I$, a crucial parameter in six-port reflectometers is the dynamic range of the power measured by the detectors $D_{P,i}$ $(i = 3, 4, 5, 6)$. It can be derived using the circle centers' distribution, as shown in the following equation [4]:

$$D_{P,i} = \left|\frac{|c_i| + 1}{|c_i| - 1}\right|. \tag{8}$$

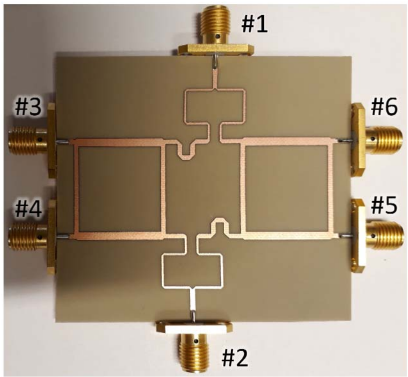


Fig. 5. Photograph of the developed balanced six-port network.

Taking (2) and (6) into account, the power dynamic range can be expressed for the proposed six-port as a function of the detectors' reflection coefficient $\Gamma_D$

$$D_{P,i} = \left|\frac{1+|\Gamma_D|}{1-|\Gamma_D|}\right| \tag{9}$$

which is shown in Fig. 4 (red curve). From this point of view, a worse impedance match of the detectors is advantageous since it enhances the power measurement dynamic range. It is due to the fact that, in the proposed balanced six-port reflectometer, the signal reflected from power detectors propagates to DUT and is reflected and travels back to the power detectors. Hence, the higher the magnitude of the reflection coefficient $\Gamma_D$ is, the higher the signal reflected from DUT.

Both the above aspects show that the proposed balanced six-port reflectometer can successfully operate with non-matched detectors. To compare the proposed structure to other reported solutions, the circle centers' distribution can be considered. In the literature, a great number of six-ports are proposed, which are characterized by $|c_i| \approx 2$. In many works, this value is considered to be optimal with respect to the measurement uncertainty although, in [15] and [4], the six-ports with smaller values of $|c_i|$ are also proposed. To show that the proposed six-port reflectometer can provide similar power handling, the following example can be given. Assuming that the reflection coefficient's magnitude $|\Gamma_D|$ is equal to $-3$ dB, the corresponding values of $|c_i|$ equal 2. This, in turn, provides a 3-dB drop between the powers delivered to the detectors with respect to the power incident, which is negligible considering the dynamic range of modern power detectors. Furthermore, the obtainable power measurement dynamic range for such $|\Gamma_D|$ is equal to 9.5 dB, which is sufficient for precise measurement, since it is also the dynamic range of power detectors in all six-port reflectometers with matched detectors, in which $|c_i| = 2$. Hence, even though the utilized power detectors are poorly matched, they can be efficiently used in the proposed reflectometer with no matching networks.

It should be underlined that, although the analysis given above is focused on a single frequency, it is valid for a wider bandwidth within which power dividers $PD_1$ and $PD_2$, directional couplers $Q_1$ and $Q_2$, and phase shifters $PS_1$ and $PS_2$ exhibit constant parameters. On the other hand, the power

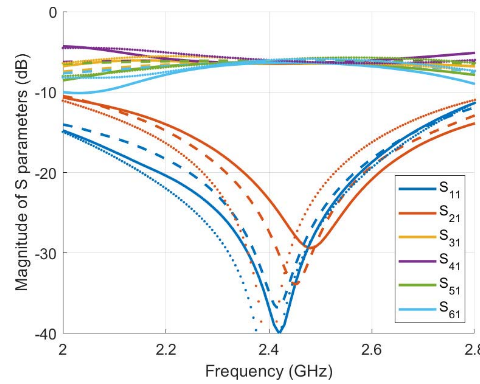


(a)

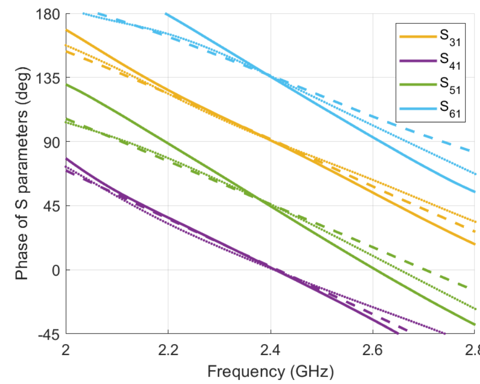


(b)

Fig. 6. Scattering parameters of the designed six-port network (a) magnitudes and (b) phases. Solid lines represent measurement results, dashed lines show results of electromagnetic calculations, and dotted lines indicate results of circuit simulation with ideal components.

detectors' reflection coefficients can vary with the frequency of operation with no deterioration of the entire reflectometer. It is only required that these reflection coefficients should be possibly close to each other at each frequency, which can easily be achieved by applying four power detectors of the same type.

## IV. Design of the Proposed Six-Port Reflectometer

The proposed balanced six-port reflectometer has been designed to operate at the frequency of 2.4 GHz. The six-port network has been designed in a microstrip structure utilizing Alon 25N substrate, characterized by a thickness of 0.508 mm and the relative permittivity equal to $\varepsilon_r = 3.38$ with $\tan\delta = 0.0025$. The power dividers $PD_1$ and $PD_2$ have been realized as the Wilkinson power dividers, and the directional couplers $Q_1$ and $Q_2$ have been designed as branch-line couplers, whereas the power shifters $PS_1$ and $PS_2$ have been realized as a section of the transmission line. For an initial verification, the six-port network has been fabricated as a separate network, i.e., with no power detectors connected. Fig. 5 shows a photograph of the manufactured six-port network, whereas a comparison of the measured scattering parameters of the manufactured network against the ones obtained from circuit simulation with the use of ideal elements and the values calculated electromagnetically is illustrated in Fig. 6. As can be observed, the six-port network provides equal power split from port #1 to ports #3–#6, to which power detectors are

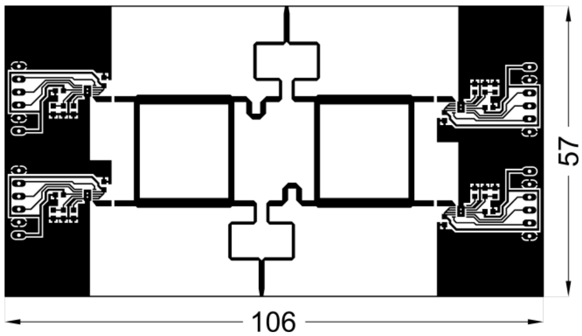


Fig. 7. Layout of the developed balanced six-port reflectometer with nonmatched power detectors.

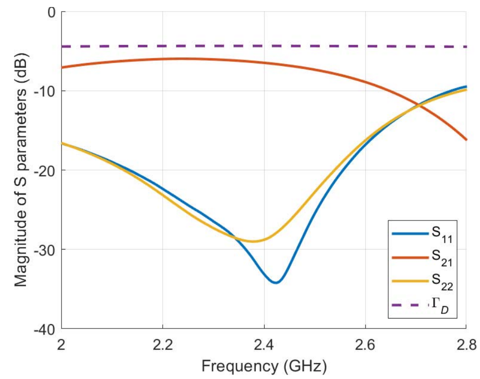


Fig. 8. Scattering parameters of the manufactured balanced six-port reflectometer and the reflection coefficient of the utilized power detectors $\Gamma_D$.

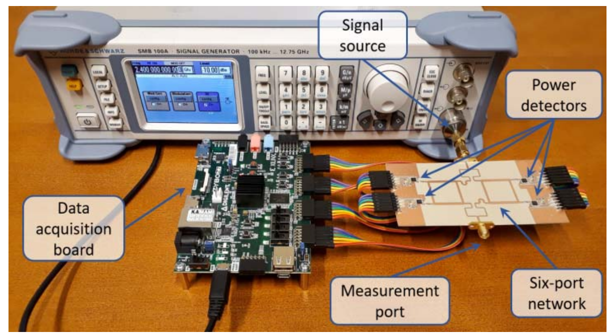


Fig. 9. Photograph of the setup for reflection coefficient measurement incorporating the developed balanced six-port reflectometer.

to be connected. On the other hand, the phase responses for the mentioned ports differ by 90° according to the theoretical assumptions. Simultaneously, very good isolation between feeding port #1 and measurement port #2 exists. The remaining scattering parameters corresponding to port #2 due to symmetry are equal to

$$S_{22} = S_{11} \tag{10a}$$

$$S_{32} = S_{51} \tag{10b}$$

$$S_{42} = S_{61} \tag{10c}$$

$$S_{52} = S_{31} \tag{10d}$$

$$S_{62} = S_{41}. \tag{10e}$$

In the next step, four LTC5587 integrated rms power detectors by Analog Devices have been connected to ports #3–#6 of the designed six-port network, forming the final layout of the designed reflectometer illustrated in Fig. 7. At the frequency of interest, these detectors provide 40 dB of the measured power dynamic range and the reflection coefficient's magnitude of −4.3 dB. Moreover, they are equipped with 12-b successive approximation ADC with a resolution of 0.014 dB/bit. The complete six-port reflectometer's layout has been manufactured, and the power detectors have been soldered. It is worth noting that the power dividers $PD_1$ and $PD_2$ operate at even excitation; therefore, the resistors that connect output ports of the Wilkinson power dividers are not obligatory to be soldered. The obtained reflectometer has been examined with the aid of a vector network analyzer. Since, to ports #3–#6, the power detectors are connected, only characterization for ports #1 and #2 is now possible. The measured reflection coefficients at these ports, the transmission between them, and the power detectors' reflection coefficient $\Gamma_D$ are depicted in Fig. 8. As seen, the obtained results clearly correspond to the theoretical predictions. Due to the balanced structure of the six-port network and the application of four identical nonmatched power detectors, the reflectometer exhibits a very good impedance match at the feeding and measurement ports. At the same time, the transmission between ports #1 and #2 occurs allowing for the manufactured reflectometer to be utilized in reflection coefficient measurements.

## V. Experimental Verification

The developed six-port reflectometer has been incorporated in a setup intended for reflection coefficient measurement. To feed port #1 of the reflectometer with −10 dBm of power a microwave signal source SMB100A by Rohde & Schwarz has been used. In addition, to read ADC data and transfer it to PC, ZYBO Z7 FPGA board by Digilent has been utilized. A photograph showing the entire measurement setup is shown in Fig. 9. Since the detectors exhibit nonlinearity exceeding ±0.5 dB, they have been calibrated by creating a lookup table containing the measured values of power for the power from signal source swept from −30 dBm to 0 dB with 0.2-dB steps. The calibration has been done for power detectors mounted in the reflectometer, for each one separately. Furthermore, all power readings have been corrected accordingly to improve the power measurement linearity.

In the next step, the developed reflectometer has been calibrated following the method reported in [25]. It is a numerical procedure that utilizes a number of one-ports with known reflection coefficients. The used one-port are matched load, open-circuit, short-circuit, and open- and short-circuits with an offset ensuring ∼90° of the reflection coefficient's phase shift, to obtain maximum diversity of reflection coefficients and, therefore, good numerical conditioning. The obtained results in the form of circle centers' distribution are illustrated in Fig. 10. As seen, the angular separation between $c_i$ points is close to the ideal one, as its deviation from 90° does not exceed 8°. On the other hand, the expected value of the magnitudes $|c_i|$ for the detectors' reflection coefficient equal to −4.3 dB is 1.64, whereas the values obtained in calibration take values between 2.17 and 2.39. This discrepancy results from insertion

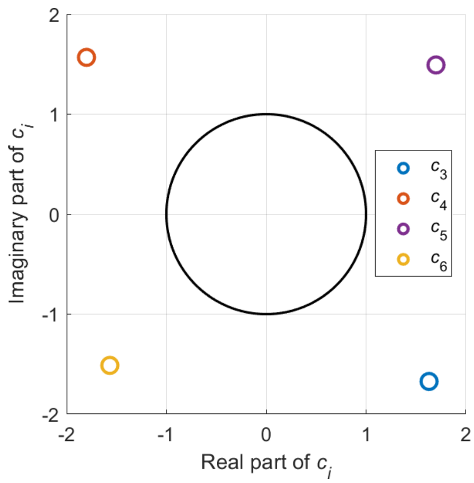


Fig. 10. Circle centers' distribution at the center frequency of 2.4 GHz obtained during the manufactured reflectometer's calibration.

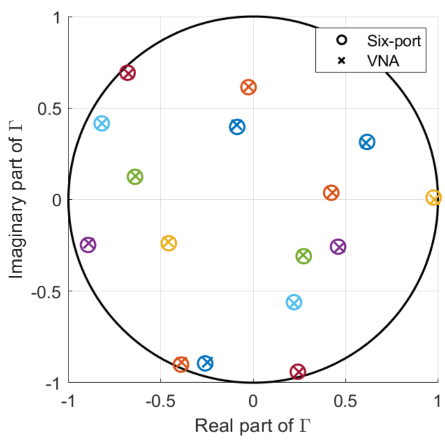


Fig. 11. Reflection coefficients of 16 reflective one-ports measured utilizing the developed six-port reflectometer and with the use of the vector network analyzer.

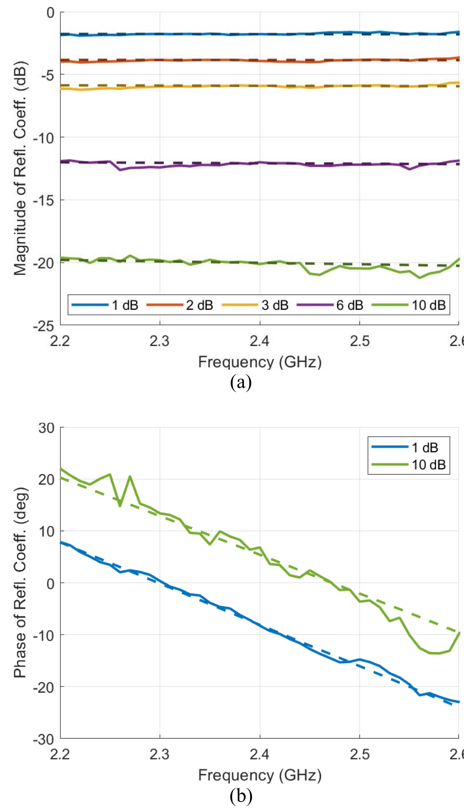


Fig. 12. Reflection coefficients of broadband SMA attenuators terminated with short-circuit, measured utilizing the developed reflectometer (solid lines) and with the use of the vector network analyzer (dashed lines). (a) Magnitudes. (b) Phases.

loss in the six-port network. It must be underlined that the signal that reflects from power detectors, propagates to DUT, is reflected, and propagates backward is more attenuated than the signal propagating from the signal source directly to the power detectors. As a consequence, the reference signal's power becomes higher in comparison to the signal related to the reflection coefficient Γ, which manifests itself in an increase in $|c_i|$ values with respect to the ones determined for the lossless six-port network. Nevertheless, this increase is not significant and does not lead to an impairment of the reflectometer's performance since the measured power takes values from $-23.7$ to $-14.4$ dB. Hence, the power dynamics range equals 9.3 dB, which is a typical value for six-port reflectometers.

To validate the developed six-port reflectometer, it has been used for reflection coefficient measurements. A set of 16 reflective one-ports has been utilized as a subject to measure. For reference, an N5224A vector network analyzer by Keysight has been used. The measurement results obtained using both the developed six-port reflectometer and the vector network analyzer are depicted in Fig. 11. The rms error equals 0.0082, whereas the maximum error is equal to 0.0122, which proves the usability of the developed balanced six-port reflectometer. For further verification in a wider range of the reflection coefficient's magnitude, a set of five SMA attenuators terminated with short-circuit has been measured. Their attenuations equal 1, 2, 3, 6, and 10 dB, which corresponds to the measured reflection coefficient's magnitudes varying from $-2$ to $-20$ dB. The measurement results compared against the values measured with the use of a vector network analyzer are indicated in Fig. 12. Due to the similar phase response of the measured attenuators, the measured reflection coefficient's phase is shown for 1- and 10-dB attenuators only. The maximum measurement error at the center frequency varies from 0.0019 dB/0.16° for the 1-dB attenuator to 0.1 dB/1.4° for the 10-dB attenuator. The corresponding error values averaged over the bandwidth from 2.2 to 2.6 GHz are equal to 0.06 dB/0.57° and 0.26 dB/1.76°, respectively. The main contributors to the measurement error are the limited length of the utilized lookup tables for power detectors' calibration and the uncertainty of the vector network analyzer used for reference measurement, which is equal to ±0.2 dB/ ±1.5° for reflection coefficients with unitary magnitude.

Furthermore, to show the advantages of the developed six-port reflectometer, it has been compared against other reported solutions in Table I. It is shown that the proposed reflectometer features the lowest design complexity as it is composed of a simple passive six-port network and does not require any matching networks for power detectors. Simultaneously, it provides low measurement error over the entire bandwidth.

TABLE I
COMPARISON OF MULTIPORT REFLECTOMETERS' PERFORMANCE

| Parameter | [4] | [5] | [6] | [9] | [11] | [17] | [18] | This work |
|---|---|---|---|---|---|---|---|---|
| Application | general purpose | general purpose | permittivity sensor | CW radar | communication receiver | CW radar | general purpose | general purpose |
| Freq. range (GHz) | 2.5-3.5 | 55-65 | 1.9-2.08, 15.2-16.6 | 24 | 2.45 | 75-84 | 1-10 | 2.2-2.6 |
| Bandwidth ratio ($f_2/f_1$) | 1.4 | 1.18 | 1.09 | 1 | 1 | 1.12 | 10 | 1.18 |
| Technology | PCB, stripline | MHMIC | MEMS | PCB, microstrip | PCB, microstrip | SiGe MMIC | PCB, microstrip | PCB, microstrip |
| Size (mm×mm) | 56×49 | 15×15 | 6.8×50 with VCO, pow. det., sensor | - | - | 1.03×1.13 with pow. det., LNA | - | 106×57 with pow. det. |
| Topology | multi-detector | multi-detector | multi-state reflectometer | multi-detector | multi-detector | multi-detector | multi-detector | multi-detector |
| No of pow. detectors | 4 | 4 | 1 | 4 | 2 | 4 | 2 | 4 |
| Measurement error (EVM) | 0.4% max | 1.7% avg | 4.5% RMS | - | 8% RMS | - | 4% max | 1.1% avg |
| Power detectors' matching networks | yes | yes | yes | yes | yes | yes | yes | no |
| Design complexity | medium | medium | high | medium | medium | high | medium | low |

It should be emphasized that the lowest measurement error is reported for the reflectometer in [4], which, however, makes use of four high-class power meters. On the other hand, all remaining reflectometers utilize simple diode detectors, for which the linearity and noise suppression are worse. In this group, the developed six-port reflectometer exhibits the lowest measurement error.

## VI. INVESTIGATION ON POWER DETECTORS' ASYMMETRY

The theoretical analysis presented in Section III is based on the assumption that all four power detectors utilized in the measurement system are identical. However, in practical realization, power detectors obviously differ slightly due to manufacturing spread. Nevertheless, as shown in Section V, the developed measurement system provides good performance that corresponds with theoretical predictions even though the four used power detectors are not identical. In the case of larger differences between the power detectors, the signal flow in the circuit would become asymmetrical, which could degrade the measurement performance. To comprehensively investigate the proposed six-port reflectometer, the detectors' asymmetry impact on the measurement performance is analyzed theoretically and experimentally in this section.

First, the detector's asymmetry can be analyzed theoretically. For this purpose, the reflectometer's parameters have been derived numerically assuming that the reflection coefficients of the power detector connected to ports #4–#6 are equal to the nominal reflection coefficient $\Gamma_{\text{Dnom}}$ of the utilized power detectors LTC5587 by Analog Devices, whereas the reflection coefficient of the power detector connected to port #3 is equal to

$$\Gamma_{D3} = \Gamma_{\text{Dnom}} + \Gamma_{\text{dev}} \tag{11}$$

where $\Gamma_{\text{dev}}$ is the deviation from the nominal reflection coefficient. The simulation has been performed assuming the magnitude $|\Gamma_{\text{dev}}|$ is equal to 0.1, 0.2, and 0.3. For each magnitude of $\Gamma_{\text{dev}}$, eight equally spaced phase values have been chosen. As a result, 24 deteriorated values of the reflection coefficient of the power detector connected to port #3 have been used to derive calibration parameters, namely, circle centers' distribution $c_i$ and the coefficients $q_i$, which relate the DUT's reflection coefficient and the measured power, as indicated by (1) and (2). The obtained results are plotted in Fig. 13. It can be observed that the deviation of a single power detector's reflection coefficient deteriorates circle centers related to the remaining power detectors, i.e., $c_4$–$c_6$. However, even for distinct values of $\Gamma_{\text{dev}}$ the circle centers' distribution is composed of four reasonably located points; therefore, its impact on the measurement quality is not significant.

On the other hand, the coefficient $q_3$ for the assumed values of $\Gamma_{\text{dev}}$ varies from 0.057 to 0.122. This, according to (1), leads to a 3.3-dB variation of the power measured by the power detector $P_3$. As discussed in Section III, such power variation is insignificant with respect to the power dynamic range of modern power detectors. Furthermore, the coefficients $q_4$–$q_6$ corresponding to the ports with the power detectors having nominal reflection coefficients remain unchanged.

The above theoretical analysis reveals that the proposed six-port reflectometer can operate properly under a distinct asymmetry of the power detectors. To validate this statement, the developed reflectometer has been modified deteriorating the reflection coefficient of the power detector $P_3$. It has been achieved by replacing the decoupling capacitor at the input of the power detector $P_3$ for the one having a capacitance of 2.2 pF, which provides 30 Ω of series reactance. The remaining power detectors $P_4$–$P_6$ are decoupled with the use of 10-nF capacitors, the reactance of which is significantly below 1 Ω. Such impaired reflectometer has been calibrated

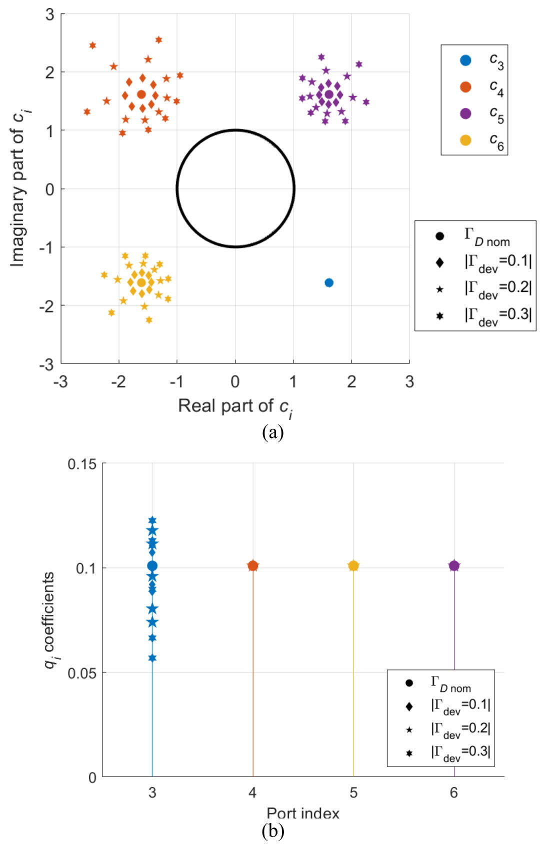


Fig. 13. Impact of the deviated reflection coefficient of the power detector $P_3$ on the six-port reflectometer's calibration parameters: (a) circle centers' distribution and (b) coefficients $q_i$.

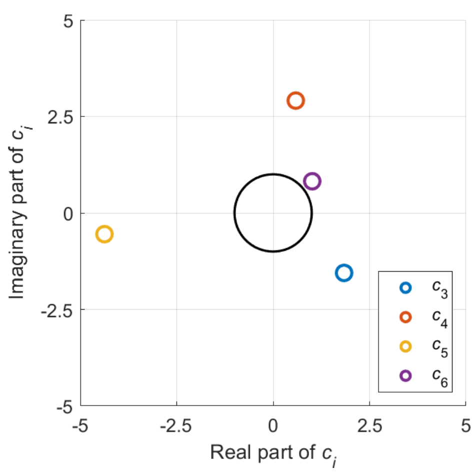


Fig. 14. Circle centers' distribution at the center frequency of 2.4 GHz obtained during the calibration of the manufactured reflectometer with the decoupling capacitor of the power detector $P_3$ replaced for the one having the capacitance of 2.2 pF.

again following the same procedure, as described in Section V; however, in this case, due to modification of the power detector $P_3$, the power detectors' calibration has not been used. The obtained circle centers' distribution is illustrated in Fig. 14. As can be observed, circle centers $c_4$–$c_6$ have deteriorated, whereas circle center $c_3$ remains unaffected, which fully corresponds to theoretical predictions. Although the overall circle centers' distribution has changed, it still allows for a correct measurement; however, the measurement accuracy may become slightly worse.

TABLE II

COMPARISON OF THE COEFFICIENTS $q$ OBTAINED IN CALIBRATION OF THE DEVELOPED SIX-PORT REFLECTOMETER IN NOMINAL STATE WITH AND WITHOUT POWER DETECTORS' CALIBRATION AND WITH MODIFIED INPUT REFLECTION COEFFICIENT OF THE POWER DETECTOR $\Gamma_{D3}$

| Reflectometer state | Power detectors' calibration | $q_3$ | $q_4$ | $q_5$ | $q_6$ |
|---|---|---|---|---|---|
| Nominal | Yes | 0.1012 | 0.1008 | 0.0947 | 0.1046 |
| Nominal | No | 0.0145 | 0.0187 | 0.0146 | 0.0158 |
| Modified $\Gamma_{D3}$ | No | 0.0061 | 0.0251 | 0.0150 | 0.0199 |

To complete the analysis of the calibration results, the coefficients $q$ must be verified. Their values can be interpreted as scaling factors relating distance on the complex plane $\Gamma$ with the measured power; hence, they are indicators of power detectors' sensitivity. The values of these coefficients have been calculated for the nominal state of the developed (i.e., with all power detectors unaffected) with and without power detectors' calibration, and for the reflectometer with modified decoupling capacitor of the power detector $P_3$. The results are listed in Table II. The values obtained for the nominal state with the power detectors calibrated are very close to 0.1. It is a consequence of the power detectors' calibration done *in situ*, which incorporates insertion losses of the six-port network. Moreover, as indicated in Section V, the power delivered from the signal source equals $-10$ dBm (0.1 mW). The coefficients $q$ obtained in the calibration without power detectors' calibration are significantly lower, as the insertion losses of the six-port network are no longer taken into account. Moreover, the spread along these values is clearly larger, which reveals part-to-part differences in power detectors' sensitivity. Finally, it is seen that, after modification of the input reflection of the power detector $\Gamma_{D3}$, the coefficient $q_3$ becomes distinctly lower than the remaining ones. Its value equals 1/3 of the averaged coefficients $q_4$–$q_6$, leading to a drop of the power measured by the detector $P_3$ by $\sim$4.8 dB with respect to power detectors $P_4$–$P_6$. Such power drop is not significant compared to the power detectors' dynamics range and should have a limited impact on the measurement capability of the developed six-port reflectometer.

In the next step, the six-port reflectometer with a modified input reflection coefficient of the power detector $\Gamma_{D3}$ has been used to perform the same measurements, as described in Section V, i.e., 16 one-ports have been measured at the center frequency (see Fig. 15), and magnitudes and phases of five attenuators terminated with short-circuit (see Fig. 16). As seen, even though the impaired six-port reflectometer exhibits degraded circle centers' distribution, it is capable of correct measurement. Nevertheless, the measurement error is distinctly higher. Detailed measurement error values are listed in Table III. It is seen that, with the modification of the

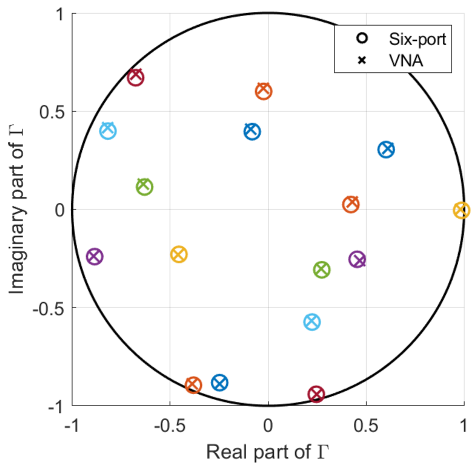


Fig. 15. Reflection coefficients of 16 reflective one-ports measured utilizing the manufactured reflectometer with the decoupling capacitor of the power detector $P_3$ replaced for the one having a capacitance of 2.2 pF and with the use of the vector network analyzer.

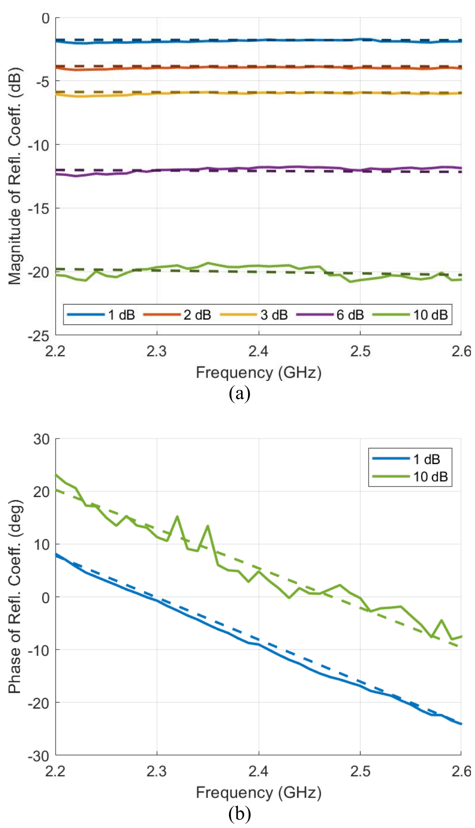


Fig. 16. Reflection coefficients of broadband SMA attenuators terminated with short-circuit, measured utilizing the manufactured reflectometer with the decoupling capacitor of the power detector $P_3$ replaced for the one having a capacitance of 2.2 pF (solid lines) and with the use of the vector network analyzer (dashed lines). (a) Magnitudes. (b) Phases.

reflection coefficient of the power detector $\Gamma_{D3}$ and with no power detectors' calibration, the error vector magnitudes at the center frequency increase by 40%. Over a wider bandwidth from 2.2 to 2.6 GHz, the magnitude and phase measurement errors also become larger. The highest increase equal to 83% is observed for the magnitude error in the case of a 2-dB

TABLE III

MEASUREMENT ERROR COMPARISON FOR THE DEVELOPED SIX-PORT REFLECTOMETER IN NOMINAL STATE AND WITH MODIFIED INPUT REFLECTION COEFFICIENT OF THE POWER DETECTOR $\Gamma_{D3}$

| Reflectometer state | Power detectors' calibration | Nominal state | Modified $\Gamma_{D3}$ |
|---|---|---|---|
| Error vector magnitude @ $f_0$ | Average | 0.008 | 0.011 |
| | Maximum | 0.012 | 0.017 |
| Average magnitude error over bandwidth 2.2 – 2.6 GHz | 1-dB attenuator | 0.06 | 0.10 |
| | 2-dB attenuator | 0.07 | 0.13 |
| | 3-dB attenuator | 0.11 | 0.10 |
| | 6-dB attenuator | 0.15 | 0.23 |
| | 10-dB attenuator | 0.26 | 0.38 |
| Average phase error over bandwidth 2.2 – 2.6 GHz | 1-dB attenuator | 0.57 | 0.86 |
| | 2-dB attenuator | 0.59 | 0.79 |
| | 3-dB attenuator | 0.85 | 0.88 |
| | 6-dB attenuator | 1.12 | 1.56 |
| | 10-dB attenuator | 1.76 | 1.77 |

attenuator, as this error increases from 0.07 to 0.13 dB, which, however, is still considerably small.

## VII. CONCLUSION

In this article, a six-port reflectometer has been presented, which incorporates four nonmatched power detectors. Due to the balanced topology of the six-port network, the signals reflected from poorly matched power detectors are efficiently utilized to form signal incident to DUT. As a result, no matching networks for power detectors are required. Simultaneously, the presented six-port reflectometer exhibits a good measurement performance as its circle center's distribution is close to the one considered in the literature to be the optimum. The proposed reflectometer has been investigated theoretically in order to verify the impact of the power detectors' match on the measurement performance. The six-port reflectometer operating at 2.4 GHz has been designed, manufactured, and incorporated in the reflection coefficient measurements providing the measurement results very close to those obtained with a commercial vector network analyzer.

Furthermore, the impact of power detectors' asymmetry has been analyzed theoretically and validated using the manufactured reflectometer with intentional impairment of the single power detector. The obtained calibration and measurement results clearly show insignificant deterioration of the measurement performance even for severe asymmetry of the power detectors. Finally, it is shown that the proposed reflectometer is capable of correct measurements over the bandwidth from 2.2 to 2.6 GHz. The impedance match of the power detectors over this bandwidth in other reported reflectometers cannot be achieved using a single stub or single *LC* section. Therefore, more complex networks must be designed, leading to an increase in the occupied area. The proposed reflectometer eliminates the need for matching networks application, which makes it suitable, e.g., for integrated microwave circuits, in which the physical size is of great importance.

## REFERENCES

[1] G. F. Engen, "The six-port reflectometer: An alternative network analyzer," *IEEE Trans. Microw. Theory Techn.*, vol. MTT-25, no. 12, pp. 1075–1080, Dec. 1977.

[2] F. M. Ghannouchi, A. Mohammadi, *The Six-Port Technique With Microwave and Wireless Applications*. Norwood, MA, USA: Artech House 2009.

[3] S. O. Tatu, A. Serban, M. Helaoui, and A. Koelpin, "Multiport technology: The new rise of an old concept," *IEEE Microw. Mag.*, vol. 15, no. 7, pp. 34–44, Nov. 2014.

[4] K. Staszek, S. Gruszczynski, and K. Wincza, "Six-port reflectometer providing enhanced power distribution," *IEEE Trans. Microw. Theory Techn.*, vol. 64, no. 3, pp. 939–951, Mar. 2016.

[5] K. Haddadi and T. Lasri, "Forward V-band vector network analyzer based on a modified six-port technique," in *Proc. IEEE Top. Conf. Wireless Sensors Sensor Netw. (WiSNet)*, San Diego, CA, USA, Jan. 2015, pp. 25–28.

[6] K. Kim, N. Kim, S.-H. Hwang, Y.-K. Kim, and Y. Kwon, "A Miniaturized broadband multi-state reflectometer integrated on a silicon MEMS probe for complex permittivity measurement of biological material," *IEEE Trans. Microw. Theory Techn.*, vol. 61, no. 5, pp. 2205–2214, May 2013.

[7] R. Mirzavand, M. M. Honari, and P. Mousavi, "Direct-conversion sensor for wireless sensing networks," *IEEE Trans. Ind. Electron.*, vol. 64, no. 12, pp. 9675–9682, Dec. 2017.

[8] C. Will *et al.*, "Segmental polynomial approximation based phase error correction for precise near field displacement measurements using Six-Port microwave interferometers," in *Proc. IEEE Top. Conf. Wireless Sensors Sensor Netw. (WiSNet)*, Phoenix, AZ, USA, Jan. 2017, pp. 23–25.

[9] G. Vinci *et al.*, "Six-port radar sensor for remote respiration rate and heartbeat vital-sign monitoring," *IEEE Trans. Microw. Theory Techn.*, vol. 61, no. 5, pp. 2093–2100, May 2013.

[10] A. O. Olopade, A. Hasan, and M. Helaoui, "Concurrent dual-band six-port receiver for multi-standard and software defined radio applications," *IEEE Trans. Microw. Theory Techn.*, vol. 61, no. 12, pp. 4252–4261, Dec. 2013.

[11] K. Haddadi, M. M. Wang, C. Loyez, D. Glay, and T. Lasri, "Four-port communication receiver with digital IQ-regeneration," *IEEE Microw. Wireless Compon. Lett.*, vol. 20, no. 1, pp. 58–60, Jan. 2010.

[12] Y. Zhang, G. Colef, Y. Li, and G. Eichmann, "Six-port optical reflectometer," *IEEE Trans. Instrum. Meas.*, vol. 40, no. 5, pp. 869–871, Oct. 1991.

[13] R. Halir *et al.*, "Integrated optical six-port reflectometer in silicon on insulator," *J. Lightw. Technol.*, vol. 27, no. 23, pp. 5405–5409, Dec. 1, 2009.

[14] A. Koelpin, G. Vinci, B. Laemmle, D. Kissinger, and R. Weigel, "The six-port in modern society," *IEEE Microw. Mag.*, vol. 11, no. 7, pp. 35–43, Dec. 2010.

[15] K. Staszek, S. Gruszczynski, and K. Wincza, "Theoretical limits and accuracy improvement of reflection-coefficient measurements in six-port reflectometers," *IEEE Trans. Microw. Theory Techn.*, vol. 61, no. 8, pp. 2966–2974, Aug. 2013.

[16] G. F. Engen, "A (historical) review of the six-port measurement technique," *IEEE Trans. Microw. Theory Techn.*, vol. 45, no. 12, pp. 2414–2417, Dec. 1997.

[17] B. Laemmle, G. Vinci, L. Maurer, R. Weigel, and A. Koelpin, "A 77-GHz SiGe integrated six-port receiver front-end for angle-of arrival detection," *IEEE J. Solid-State Circuits*, vol. 47, no. 9, pp. 1966–1973, Sep. 2012.

[18] K. Haddadi, M. M. Wang, D. Glay, and T. Lasri, "Ultra wide-band four-port reflectometer using only two quadratic detectors," in *IEEE MTT-S Int. Microw. Symp. Dig.*, Atlanta, GA, USA, Jun. 2008, pp. 379–382.

[19] J. Monzo-Cabrera, J. L. Pedreno-Molina, A. Lozano-Guerrero, and A. Toledo-Moreo, "A novel design of a robust ten-port microwave reflectometer with autonomous calibration by using neural networks," *IEEE Trans. Microw. Theory Techn.*, vol. 56, no. 12, pp. 2972–2978, Dec. 2008.

[20] K. Staszek, S. Gruszczynski, and K. Wincza, "Broadband ten-port reflectometer with enhanced measurement accuracy," in *Proc. IEEE 16th Annu. Wireless Microw. Technol. Conf. (WAMICON)*, Cocoa Beach, FL, USA, Apr. 2015, pp. 1–4.

[21] K. Haddadi and T. Lasri, "Formulation for complete and accurate calibration of six-port reflectometer," *IEEE Trans. Microw. Theory Techn.*, vol. 60, no. 3, pp. 574–581, Mar. 2012.

[22] S. Linz *et al.*, "I/Q imbalance compensation for six-port interferometers in radar applications," in *Proc. 44th Eur. Microw. Conf.*, Rome, Italy, Oct. 2014, pp. 6–9.

[23] S. Julrat and S. Trabelsi, "Portable six-port reflectometer for determining moisture content of biomass material," *IEEE Sensors J.*, vol. 17, no. 15, pp. 4814–4819, Aug. 2017.

[24] S. Mann *et al.*, "Diode detector design for 61 GHz substrate integrated waveguide six-port radar systems," in *Proc. IEEE Topical Conf. Wireless Sensors Sensor Netw. (WiSNet)*, San Diego, CA, USA, Jan. 2015, pp. 44–46.

[25] K. Staszek, P. Kaminski, A. Rydosz, S. Gruszczynski, and K. Wincza, "A least-squares approach to the calibration of multiport reflectometers," in *IEEE MTT-S Int. Microw. Symp. Dig.*, New Delhi, India, Dec. 2013, pp. 1–4.

**Kamil Staszek** received the M.Sc., Ph.D., and D.Sc. (Habilitation) degrees in electronics engineering from the AGH University of Science and Technology, Krakow, Poland, in 2011, 2015, and 2019, respectively.

He is currently an Associate Professor with the Department of Electronics, AGH University of Science and Technology. He has more than two years of industrial experience in automotive radars development. He has coauthored more than 70 journal articles and conference scientific papers. His main scientific research interests include multiport measurement techniques in sensor applications and the design of broadband passive components.

Dr. Staszek is a member of the Technical Program Committee of the International Conference on Microwaves, Radar, and Wireless Communications (MIKON) and the Junior Vice-Chair of the Polish Section of the International Union of Radio Science (URSI)-Commission A.